

Complex Adaptive Systems, Volume 1
Cihan H. Dagli, Editor in Chief
Conference Organized by Missouri University of Science and Technology
2011- Chicago, IL

Gravity compensation in accelerometer measurements for robot navigation on inclined surfaces

Jonathan R. Nistler, Majura F. Selekwa*

Department of Mechanical Engineering, North Dakota State University Dept 2490, P.O. Box 6050, Fargo, ND, 58108-6050

Abstract

Accelerometers are used in most robot navigation systems as sensors for robot speed and localization. Normally, these accelerometers sense the body acceleration, which is integrated to determine the robot velocity, and cumulatively the robot position relative to the starting position. When the robot is moving on a horizontal surface, the computed speed will in general reflect the actual robot speed; however, when the robot is moving on an inclined surface, such as uphill or downhill motions, then the measured speed will include components due to gravity, which are not part of the actual robot speed. Therefore the computed speed will not reflect the actual robot speed. These gravity components must be compensated for in the speed computations to capture the actual robot speed. This paper proposes a computational approach for elimination of the gravity components from the accelerometer measurements using a 3-axis accelerometers combined with 3-axis gyro on tilted surfaces. The compensated accelerometer speed results were compared to simulated robot speed results on inclined surfaces, and were found to accurately reflect the actual robot speed. By using these compensated accelerometer results it becomes possible to determine the robot speed even under wheel slip conditions.

©2011 Published by Elsevier B.V. Open access under [CC BY-NC-ND license](#).

Keywords: Odometry, mobile robots, gravity compensation, accelerometers, IMU.

1. Introduction

In robotic vehicle applications, the ability for the robot to self understand its location in space is critically important for successful accomplishment of its mission. Robot localization requires a good odometry system, which can have various types of sensors that track the motion of the vehicle. Among the popular sensors used by many odometry systems include wheel encoders that track the vehicle motion by monitoring the rotation of its wheels, inertial measurement units (IMU) that combine accelerometers for monitoring the acceleration of the vehicle and gyros for

*Corresponding Author

Email addresses: Jonathan.R.Nistler@ndsu.edu (Jonathan R. Nistler), majura.selekwa@ndsu.edu (Majura F. Selekwa)

monitoring the rate of change of the vehicle orientation [1, 2]. Certain systems include a global position system (GPS) receiver [3, 4]; however, since the accuracy of GPS receivers tend to be unreliable when the robot is in confined environments such as indoors, underground tunnels, forests and built urban areas with high rise buildings such as urban environments, the GPS-based systems have not been very popular in many robotic applications.

Most odometry systems for robotic applications use IMUs that have accelerometer sensors. These sensors continuously monitor the acceleration of the vehicle, which is integrated to determine the speed, and the second integration yields the position relative to the starting point. Because of the influence of gravity, coriolis and rotational components of acceleration, accelerometer based odometry systems are subject to a multitude of errors depending on how the measurements are processed. To minimize these errors, most applications tend to assume that the robot is on a flat ground following a relatively straight line path. All errors that arise from employing such an assumption are treated as noise that is usually filtered using some sort of a filter [5, 6, 7, 2, 8, 9, 10, 11]. Although these methods have been sufficient for many applications, they are susceptible to intolerably larger errors when the robot is operated on an inclined path where the effect of gravity can be very significant.

This paper proposes a numerical algorithm for processing accelerometer measurements by totally eliminating the influence of gravity and other unwanted components of vehicle acceleration. The algorithm is based on standard three-dimensional kinematics of multibody systems [12, 13]. The paper is divided into five sections. Section 2 presents the basic relationship between the accelerometer measurements and the vehicle acceleration; this relationship is utilized by Section 3 to lay out a comprehensive computational algorithm for this problem. The simulation results of the proposed algorithm are presented in Section 4 before closing the paper with some concluding remarks in Section 5.

2. The Problem of Accelerometer Measurements in Odometry

Assume that the frame xyz is attached to, and moves with the vehicle at its center of mass, G , such that the y axis is always pointing in the direction of the vehicle in the XYZ inertial frame. If a three axis accelerometer equipped with

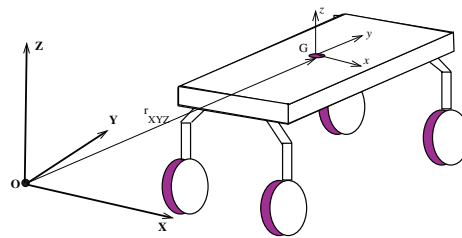


Figure 1: Kinematic configuration of accelerometer measurements in the inertial frame.

with a three axis gyro is attached to a vehicle as shown in Figure 1, then the accelerometer measurements $\ddot{\vec{r}}_{xyz}$ do not directly represent the actual acceleration of the vehicle $\ddot{\vec{r}}_{XYZ}$ in the inertial frame as required by the odometry system. It can easily be shown that that these quantities are related through

$$\ddot{\vec{r}}_{xyz} = J\ddot{\vec{r}}_{XYZ} + 2\dot{J}\dot{\vec{r}}_{XYZ} + \ddot{J}\vec{r}_{XYZ} \quad (1)$$

where matrix J is the X - Y - Z rotation matrix defined using standard Euler angles θ_x , θ_y , and θ_z as [12, 13]

$$J = \begin{bmatrix} \cos \theta_y \cos \theta_z & -\sin \theta_z \cos \theta_x + \sin \theta_x \sin \theta_y \cos \theta_z & \sin \theta_x \sin \theta_z + \cos \theta_x \sin \theta_y \cos \theta_z \\ \cos \theta_y \sin \theta_z & \cos \theta_z \cos \theta_x + \sin \theta_x \sin \theta_y \sin \theta_z & -\sin \theta_x \cos \theta_z + \cos \theta_x \sin \theta_y \sin \theta_z \\ -\sin \theta_y & \cos \theta_y \sin \theta_x & \cos \theta_x \cos \theta_y \end{bmatrix} \quad (2)$$

The accelerometer measurements include the Coriolis component, $2\dot{J}\dot{\vec{r}}_{XYZ}$, and the rotational component, $\ddot{J}\vec{r}_{XYZ}$, which are not required by the odometry system. Additionally, the vehicle inertial acceleration also includes a component due to gravity g , i.e.

$$\ddot{\vec{r}}_{XYZ} = \begin{pmatrix} \ddot{X} \\ \ddot{Y} \\ \ddot{Z} - g \end{pmatrix}. \quad (3)$$

Therefore, it is clear that the accelerometer measurements for a robotic vehicle on an irregular terrain need to be processed further if they are to be used in the robot odometry system.

Standard principles of systems dynamics and the orthonormality property of rotation matrix J leads to

$$\dot{J} = \tilde{\omega}J, \quad \ddot{J} = (\dot{\tilde{\omega}} + \tilde{\omega}^2)J, \quad (4)$$

where $\tilde{\omega}$ and $\dot{\tilde{\omega}}$ respectively are the skew symmetric angular velocity and angular acceleration matrices made of the actual axis rotation parameters as may be recorded by the three-axis gyro. These matrices are defined as

$$\tilde{\omega} = \begin{pmatrix} 0 & -\omega_z & \omega_y \\ \omega_z & 0 & -\omega_x \\ -\omega_y & \omega_x & 0 \end{pmatrix}, \quad \dot{\tilde{\omega}} = \begin{pmatrix} 0 & -\dot{\omega}_z & \dot{\omega}_y \\ \dot{\omega}_z & 0 & -\dot{\omega}_x \\ -\dot{\omega}_y & \dot{\omega}_x & 0 \end{pmatrix}, \quad (5)$$

corresponding to the angular velocity vector of the vehicle, $\Omega = [\omega_x, \omega_y, \omega_z]^T$, which represent to the pitch, roll, and yaw rates, and the angular acceleration vector, $\dot{\Omega} = [\dot{\omega}_x, \dot{\omega}_y, \dot{\omega}_z]^T$. The angular velocity vector, Ω , is related to the Euler angle rates, $\dot{\Theta} = [\dot{\theta}_x, \dot{\theta}_y, \dot{\theta}_z]^T$, through

$$\begin{pmatrix} \dot{\theta}_x \\ \dot{\theta}_y \\ \dot{\theta}_z \end{pmatrix} = \begin{pmatrix} \frac{\cos \theta_z}{\cos \theta_y} & \frac{\sin \theta_z}{\cos \theta_y} & 0 \\ -\sin \theta_z & \cos \theta_z & 0 \\ \cos \theta_z \tan \theta_y & \sin \theta_z \tan \theta_y & 1 \end{pmatrix} \begin{pmatrix} \omega_x \\ \omega_y \\ \omega_z \end{pmatrix}, \quad (6)$$

subject to angle constraints $-\frac{\pi}{2} < \theta_x, \theta_y, \theta_z < \frac{\pi}{2}$. Therefore, the actual vehicle acceleration components \ddot{X} , \ddot{Y} , and \ddot{Z} relate to the accelerometer measurements \ddot{r}_{xyz} through

$$\begin{pmatrix} \ddot{X} \\ \ddot{Y} \\ \ddot{Z} \end{pmatrix} = J^T \left[\ddot{r}_{xyz} - 2\tilde{\omega}J\dot{r}_{XYZ} - (\dot{\tilde{\omega}} + \tilde{\omega}^2)J\dot{r}_{XYZ} \right] + \underbrace{\begin{pmatrix} 0 \\ 0 \\ g \end{pmatrix}}_{g\text{-corrector}}. \quad (7)$$

These equations show that the actual relationship between the accelerometer measurements and the body accelerations is relatively more complex. Most robotics applications assume that all Euler angles have constant zero values such that the accelerometer measurements are exactly a representative of the vehicle measurements subject to the g -corrector term, which makes it easy to transform those measurements into body motion accelerations suitable for odometry applications. This assumption is normally valid in controlled laboratory environments where the terrain is perfectly flat [14], however, most field applications involve some kind of an estimation process that lump together all unmodelled dynamics as noise that is filtered out [5, 6, 7, 2, 8, 9, 10, 11] or use some sort of an expert system to perform the estimation [15].

3. Proposed Computational Approach

For notational simplicity, the vehicle body acceleration, velocity and position measurements at any discrete instant k will be represented by $\ddot{r}_{XYZ}(k)$, $\dot{r}_{XYZ}(k)$ and $r_{XYZ}(k)$ where the acceleration vector is assumed to be free of gravitational effects. Let the rotational matrix J be expressed in terms of Euler angle vector Θ at any instant k as $J_{\Theta(k)}$, and the g -corrector vector be denoted as \tilde{g} . Then, equation (7) at any instant k can be rewritten as

$$\ddot{r}_{XYZ}(k+1) = J_{\Theta(k)}^T \left[\ddot{r}_{xyz}(k) - 2\tilde{\omega}(k)J_{\Theta(k)}\dot{r}_{XYZ}(k) - (\dot{\tilde{\omega}}(k) + \tilde{\omega}^2(k))J_{\Theta(k)}\dot{r}_{XYZ}(k) \right] + \tilde{g}, \quad (8)$$

where the desired odometry data include $\dot{r}_{XYZ}(k)$ and $\ddot{r}_{XYZ}(k)$. The available measured data include the accelerometer measurements $\ddot{r}_{xyz}(k)$ and the gyro measurements $\Omega(k) = [\omega_x(k), \omega_y(k), \omega_z(k)]^T$. The Euler rates can numerically be determined using (6) as

$$\dot{\Theta}(k) = C_e(k-1)\Omega(k), \quad (9)$$

where

$$C_e(k) = \begin{pmatrix} \frac{\cos \theta_z(k)}{\cos \theta_y(k)} & \frac{\sin \theta_z(k)}{\cos \theta_y(k)} & 0 \\ -\sin \theta_z(k) & \cos \theta_z(k) & 0 \\ \cos \theta_z(k) \tan \theta_y(k) & \sin \theta_z(k) \tan \theta_y(k) & 1 \end{pmatrix}. \quad (10)$$

By using a simple backward¹ Euler rule for numerical differentiation

$$\dot{s}(k) = \frac{s(k) - x(k-1)}{\Delta\tau}, \quad (11)$$

where $\Delta\tau$ is the computational sampling interval, the Euler angles can now be computed according as

$$\Theta(k) = \dot{\Theta}(k)\Delta\tau + \Theta(k-1), \quad (12)$$

which leads to the rotational matrix $J_{\Theta(k)}$. Knowing the gyro rate measurements $\Omega(k)$, it is straightforward to determine the angular acceleration vector $\ddot{\Omega}(k+1)$, using numerical differentiation and forming angular matrices $\tilde{\omega}(k)$ and $\dot{\tilde{\omega}}(k)$.

Similarly, the vehicle speed and position can be defined as follows

$$\dot{\vec{r}}_{XYZ}(k) = \ddot{\vec{r}}_{XYZ}(k)\Delta\tau + \dot{\vec{r}}_{XYZ}(k-1) \quad (13)$$

$$\vec{r}_{XYZ}(k) = \dot{\vec{r}}_{XYZ}(k)\Delta\tau + \vec{r}_{XYZ}(k-1) \quad (14)$$

where $\ddot{\vec{r}}_{XYZ}(k)$ is defined as in (8), and is determined using a combination of all results described from (9) through (14). This process is iteratively repeated in a continuous loop as long as the robot is in motion. Although initial Euler angles do not have to be zero, it does not harm to start the iteration by assuming that they have zero values.

Table 3 shows the algorithmic listings for this numerical implementation.

Table 1: The Algorithmic listing for implementing the proposed process of reading accelerometer data

0.	Initialize, set $k = 0$
1.	\Rightarrow Set initial values of $\dot{\vec{r}}_{XYZ}(k)$, $\vec{r}_{XYZ}(k)$, $\Theta(k)$, and $\tilde{\omega}(k)$
2.	REPEAT $k \rightarrow k + 1$,
3.	\Rightarrow use $\ddot{\vec{r}}_{XYZ}(k)$ to compute $\dot{\vec{r}}_{XYZ}(k)$ and $\vec{r}_{XYZ}(k)$ \triangleright preserve $\dot{\vec{r}}_{XYZ}(k)$ and $\vec{r}_{XYZ}(k)$ DISPLAY $\dot{\vec{r}}_{XYZ}(k)$ and $\vec{r}_{XYZ}(k)$
4.	Measure $\ddot{\vec{r}}_{XYZ}(k)$, and $\Omega(k)$
5.	\Rightarrow use $\Omega(k)$ to compute $\dot{\Theta}(k)$, and $\Theta(k)$ \triangleright preserve $\Theta(k)$
6.	\Rightarrow use $\Omega(k)$ to compute $\tilde{\omega}(k)$ and $\dot{\tilde{\omega}}(k)$ \triangleright preserve $\tilde{\omega}(k)$
7.	Use $\Theta(k)$ to compute $J_{\Theta(k)}$
8.	Use available data to compute $\ddot{\vec{r}}_{XYZ}(k+1)$
9.	If not done, GOTO STEP 2

4. Simulation Results

The numerical algorithm described in Section 3 was coded in MATLAB, and used for simulating the performance of a BIBOT-1 robotic vehicle of Figure 2. This Vehicle is assumed to be equipped with four wheel encoders of 100 pulse/rev on each wheel of 0.085 meters radius, and one ITG3200/ADXL345 Digital IMU Combo Board. The IMU

¹ Better results can be obtained by using higher order numerical integration and differentiation

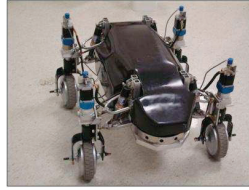


Figure 2: The structure of the experimental robotic vehicle that was numerically simulated.

include three-axis accelerometers of up to $\pm 16\text{ g}$ accelerations and three-axis gyros of up to $\pm 2000^\circ/\text{sec}$ gyro rates.

In these simulation results, the forward acceleration of the vehicle (corresponding to the y-axis) was maintained at a constant value of 0.4 m/s . The pitch and roll angles of the vehicle were varied sinusoidally as illustrated in Figure 3, which in effect changed the Euler angles as shown in Figure 4; the yaw angle was kept constant. The

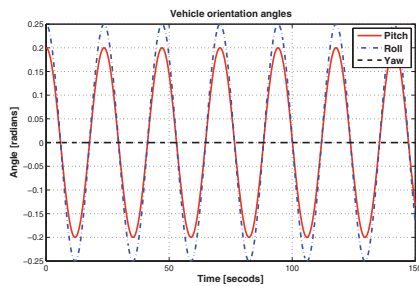


Figure 3: Simulated Vehicle orientation Angles

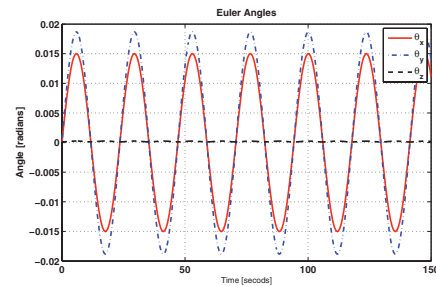


Figure 4: Resulting Vehicle Euler Angles

corresponding simulated values of the accelerometer readings for all three axes were recorded and processed using the algorithm discussed in Section 3. Figures 5 through 7 compare the processed accelerations to the simulated acceleration measurements. As seen in these results, the accelerometer measurements were sensitive to the vehicle configuration angles: the pitch and roll angles, even though the yaw angle was assumed to remain constant.

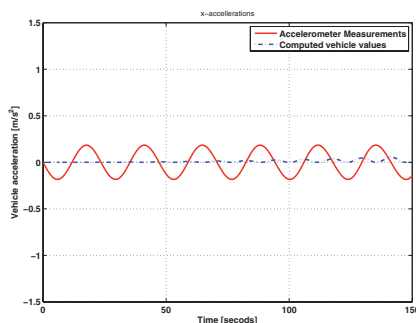


Figure 5: The Lateral x-axis accelerations.

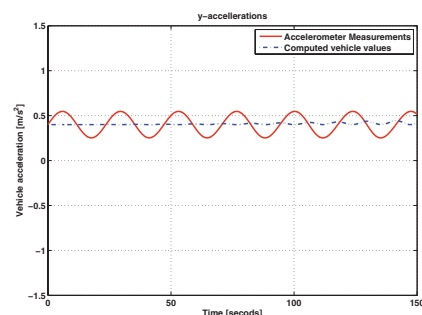


Figure 6: The longitudinal y-axis accelerations.

The speed of the vehicle computed using the processed vehicle acceleration was equal to the simulated speed, while that due to accelerometer data was not equal to the simulated speed. The vertical accelerations increased further as the speed increased because of the nature of the surface, which was very corrugated; this could be improved by increasing the corrugation wavelength. Out of space constraints, graphs comparing the accelerometer measurements and the vehicle accelerations when the vehicle was maintained at a flat surface with zero values of roll, pitch, and yaw angles will not be shown. However, when all Euler angles are maintained at zero, the two acceleration data sets were identical, indicating that the accelerometers captured the vehicle accelerations accurately.

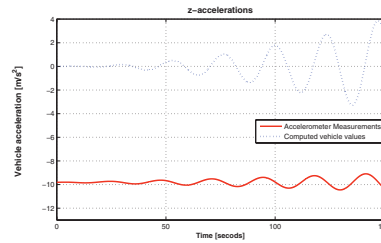


Figure 7: The vertical Z-axis accelerations.

5. Summary and Conclusions

This paper has discussed the effect of gravity, coriolis and rotational acceleration components on the accelerometer measurements used in robot odometry. A computational approach for processing accelerometer measurements into vehicle accelerations by eliminating all unwanted acceleration components that affect odometry performance was proposed. The approach is based on standard kinematics of multibody systems that involves a rotational matrix of Euler angles in transformation between the accelerometer axes and the world inertial axes. It requires measurements using a combination of a three-axis accelerometer and a three-axis gyro. Gyro measurements are used in establishing the actual Euler angles for forming the required rotation matrix that is eventually used in extracting the vehicle acceleration from the accelerometer data. Simulation results using first order integration methods have shown that, on irregular roads, the accelerometer data do not reflect the actual vehicle accelerations; and the proposed method was successful in extracting the vehicle acceleration from the accelerometer data. It is hoped that better results could be obtained by combining this computational approach with a filter. Future work on this project focuses on experimentally testing this approach on a real robot along highly irregular roads.

References

- [1] J. Borenstein, H. R. Everett, L. Feng, D. Wehe, Mobile robot positioning: Sensors and techniques, *Journal of Robotic Systems* 14 (4) (1997) 231–249.
- [2] H. Liu, G. Pang, Accelerometer for mobile robot positioning, *Industry Applications, IEEE Transactions on* 37 (3) (2001) 812–819. doi:10.1109/28.924763.
- [3] G. Reina, A. Vargas, K. Nagatani, K. Yoshida, Adaptive kalman filtering for gps-based mobile robot localization, in: *Safety, Security and Rescue Robotics, 2007. SSRR 2007. IEEE International Workshop on*, 2007, pp. 1–6. doi:10.1109/SSRR.2007.4381270.
- [4] D. Maier, A. Kleiner, Improved GPS sensor model for mobile robots in urban terrain, in: *Robotics and Automation (ICRA), 2010 IEEE International Conference on*, 2010, pp. 4385–4390. doi:10.1109/ROBOT.2010.5509895.
- [5] T. Lee, J. Shin, D. Cho, Position estimation for mobile robot using in-plane 3-axis imu and active beacon, in: *Industrial Electronics, 2009. ISIE 2009. IEEE International Symposium on*, 2009, pp. 1956–1961. doi:10.1109/ISIE.2009.5214363.
- [6] S. Tanaka, S. Nishifuji, Automatic on-line measurement of ship's attitude by use of a servo-type accelerometer and inclinometers, *Instrumentation and Measurement, IEEE Transactions on* 45 (1) (1996) 209–217. doi:10.1109/19.481336.
- [7] P. Batista, C. Silvestre, P. Oliveira, On the observability of linear motion quantities in navigation systems, *Systems & Control Letters* 60 (2) (2011) 101–110. doi:DOI: 10.1016/j.sysconle.2010.11.002.
- [8] P. Batista, C. Silvestre, P. Oliveira, Optimal position and velocity navigation filters for autonomous vehicles, *Automatica* 46 (4) (2010) 767–774. doi:DOI: 10.1016/j.automatica.2010.02.004.
- [9] J. Balaram, Kinematic observers for articulated rovers, in: *Robotics and Automation, 2000. Proceedings. ICRA '00. IEEE International Conference on*, Vol. 3, 2000, pp. 2597–2604 vol.3. doi:10.1109/ROBOT.2000.846419.
- [10] R. Toledo-Moreo, M. A. Zamora-Izquierdo, Collision avoidance support in roads with lateral and longitudinal maneuver prediction by fusing gps/imu and digital maps, *Transportation Research Part C: Emerging Technologies* 18 (4) (2010) 611–625. doi:DOI: 10.1016/j.trc.2010.01.001.
- [11] S. L. Fagin, A unified approach to the error analysis of augmented dynamically exact inertial navigation systems, *Aerospace and Navigational Electronics, IEEE Transactions on* ANE-11 (4) (1964) 234–248. doi:10.1109/TANE.1964.4502207.
- [12] H. Baruh, *Analytical Dynamics*, McGraw-Hill International, 1998.
- [13] A. A. Shabana, *Dynamics of multibody systems*, Cambridge University Press, 2005.
- [14] H.-S. Ahn, W. Yu, Indoor mobile robot and pedestrian localization techniques, in: *Control, Automation and Systems, 2007. ICCAS '07. International Conference on*, 2007, pp. 2350–2354. doi:10.1109/ICCAS.2007.4406753.
- [15] L. Ojeda, J. Borenstein, Flexnav: fuzzy logic expert rule-based position estimation for mobile robots on rugged terrain, in: *Robotics and Automation, 2002. Proceedings. ICRA '02. IEEE International Conference on*, Vol. 1, 2002, pp. 317–322 vol.1. doi:10.1109/ROBOT.2002.1013380.